ARTICLE
Journal of Cellular Biochemistry 112:1857–1868 (2011)

Journal of Cellular Biochemistry

The Activity of Aminoacyl-tRNA Synthetase-Interacting Multi-Functional Protein 1 (AIMP1) on Endothelial Cells is Mediated by the Assembly of a Cytoskeletal Protein Complex

Valentina Charlotte Jackson,* Sarah Dewilde, Alessandra Giuliano Albo, Katarzyna Lis, Davide Corpillo, and Barbara Canepa

LIMA, BioIndustry Park Silvano Fumero S.p.A., Colleretto Giacosa (TO), Italy

ABSTRACT

AIMP1 was first found as a factor associated with the aminoacyl-tRNA synthetase (ARS) complex. However, it is also secreted and acts on different target cells such as endothelial cells, macrophages, and fibroblasts as an extracellular regulator, respectively, of angiogenesis, inflammatory responses and dermal regeneration. AIMP1 has also been reported to suppress in vivo tumor growth. In this study, we investigated the signaling pathways activated by exogenous AIMP1 in an in vitro endothelial model. AIMP1 decreases EC viability through an $\alpha5\beta1$ integrin-dependent mechanism and inhibits cell adhesion, is internalized and shows an asymmetric pattern of distribution and accumulation in cell protrusions. Experiments of affinity purification, pull down, and co-immunoprecipitation showed that AIMP1 interacts with four cytoskeletal proteins (filamin-A, α-tubulin, vinculin, and cingulin). α-Tubulin also gets phosphorylated upon cell treatment with AIMP1 and colocalization between AIMP1 and filamin-A as well as between AIMP1 and cingulin was observed through immunofluorescence assays. In this work, we propose that AIMP1 effect on EC adhesion is mediated by the assembly of a cytoskeletal protein complex on the cytosolic face of the cell membrane which could regulate cellular architecture maintenance and remodeling. Moreover, this activity is able to indirectly influence cell viability. J. Cell. Biochem. 112: 1857–1868, 2011. © 2011 Wiley-Liss, Inc.

KEY WORDS: AIMP1; ENDOTHELIAL CELLS; ANGIOGENESIS; SIGNALING PATHWAY; CYTOSKELETON; ADHESION

AIMP1 (ARS-interacting multifunctional protein 1) is a cofactor of the aminoacyl-tRNA synthetase (ARS) complex which is composed of nine different enzymes and three non-enzymatic cofactors, including AIMP1 [Quevillon et al., 1997]. AIMP1 is also the precursor of EMAP II (endothelial monocyte-activating polypeptide II) [Shalak et al., 2001] which possesses a wide range of activities toward endothelial cells (ECs), neutrophils, and monocyte/macrophages in vitro [Kao et al., 1994a,b]. Interestingly, AIMP1 itself shows cytokine properties and secreted AIMP1 acts on different target cells such as monocyte/macrophages [Ko et al., 2001; Park et al., 2002a,b], ECs [Chang et al., 2002; Park et al., 2002c], and fibroblasts [Park et al., 2005b]. It activates monocytes/macrophages to induce various proinflammatory cytokines, such as tumor necrosis factor (TNF)-α, interleukin-8 (IL-8), macrophage chemotactic protein-1 (MCP-1), macrophage inflammatory protein-1α (MIP-1α), and IL-1β [Ko et al., 2001; Park et al., 2005b], and controls angiogenesis by a dual mechanism involving the migration and death of ECs [Park et al., 2002c, 2005b]. Furthermore, AIMP1, as well as EMAP II, have been reported to suppress in vivo tumor growth [Schwarz et al., 1999; Lee et al., 2006].

For EMAP II an activity on the EC actin cytoskeleton has been reported, with different effects during adhesion, in which it causes disassembly of actin network stress fibers [Schwarz et al., 2005] and in adherent cells, where intracellular actin fibers and focal adhesion are noted to be increased [Keezer et al., 2003]. Instead, a role for AIMP1 in cytoskeleton remodeling has never been investigated.

The cytoskeleton is composed of different structures, microfilaments, microtubules (MTs), and intermediate filaments (IFs) which dominate mechanical properties of cytoplasm [Janmey, 1991]. Cytoskeleton remodeling in dynamic cellular processes produces changes in cell shape and motility in response to external stimuli. It is therefore involved in signal transduction [Revenu et al., 2004] and fundamental to a variety of biological processes such as directing cell polarity, facilitating membrane and organelle traffic, cell

Grant sponsor: Bioindustry Park Silvano Fumero, Piedmont Region, ISI Foundation.

*Correspondence to: Valentina Charlotte Jackson, Valentina Jackson, Laboratorio Integrato Metodologie Avanzate (LIMA), Bioindustry Park Silvano Fumero S.p.A., Via Ribes 5, I-10010 Colleretto Giacosa (TO), Italy.
E-mail: jackson@bipcamail.it

Received 5 January 2011; Accepted 9 March 2011 • DOI 10.1002/jcb.23104 • © 2011 Wiley-Liss, Inc.
Published online 17 March 2011 in Wiley Online Library (wileyonlinelibrary.com).

adhesion, chromosome segregation, cell migration, and cell division [Pelling et al., 2007; Chesarone et al., 2010]. This process necessitates the activation of the cell motility machinery, resulting in actin cytoskeleton remodeling which requires tight spatial and temporal regulation of actin filament assembly and organization [Stossel, 1993; Sechi and Wehland, 2000]. These features of the actin cytoskeleton are regulated by a cohort of actin-associated cytoskeletal proteins (e.g., filamin, talin, vinculin, profilin, cofilin), which were initially considered to be structural components organizing a stable actin cytoskeleton, but are now known to be cellular dynamics regulators and key signaling process components [Revenu et al., 2004]. Together with the actin cytoskeleton, also MTs and IFs play an important role in the cell mechanical properties [Gundersen and Cook, 1999; Zhu et al., 2000]. MTs are found extensively throughout the cell in the cytoplasm between the nucleus and the cell membrane; they are dynamic structures, able to grow and depolymerize in response to signaling pathways and environmental conditions [Pelling et al., 2007].

Since it is not yet determined how AIMP1 exerts its complex extracellular activities, we conducted a series of in vitro experiments to investigate the signaling pathways activated by exogenous AIMP1 in ECs and proposed a cellular mechanism by which AIMP1, upon cell uptake, acts on ECs through the assembly of a protein complex composed of at least four cytoskeletal proteins on the cytosolic face of the cell membrane (α-tubulin, vinculin, cingulin, and filamin-A).

MATERIALS AND METHODS

ANTIBODIES, CHEMICALS, AND OTHER REAGENTS

Unless otherwise indicated, all chemicals, solvents, and reagents were purchased from Sigma–Aldrich Co. (St. Louis, MO).

Primary antibodies used were provided by Santa Cruz Biotechnology (Santa Cruz, CA), except for rabbit anti-pERK/ERK, anti-pJNK/JNK, and anti-pAKT/AKT antibodies which were from Cell Signalling Technology (Beverly, MA) and mouse anti-α5β1 integrin antibody from Millipore (Billerica, MA).

CELL CULTURE

The EC model used was an immortalized Porcine Aorta Endothelial Cell line (PAEC) kindly given by Prof. Bussolino (IRCC, Candiolo, TO). Cells were cultured in Ham's F-12 medium supplied with 10% fetal bovine serum (FBS), 100 μg/ml penicillin–streptomycin 10 U/μl and 2 mM glutamine in a humified 5% CO_2 incubator at 37°C.

PRODUCTION AND PURIFICATION OF RECOMBINANT AIMP1

Human AIMP1 was expressed as a His-tag fusion protein in *Escherichia coli* TOP F10 cells. The growing bacteria were harvested and resuspended in phosphate buffer (50 mM NaH_2PO_4, 300 mM NaCl, 50 μg/ml RNAse, 4 U/ml benzonase nuclease, 2 mM DTT, 0.5 mM PMSF, 1× protease inhibitor cocktail, pH 8.0), sonicated, centrifuged and purified using a Ni-Sepharose column (Ni Sepharose high performance, GE Healthcare, Uppsala, Sweden) and a Hi-Trap cationic-exchange column (Hi Trap SP HP; GE Healthcare).

In order to remove lipopolysaccharides (LPS), the protein underwent five cycles of Triton X-114 extraction [Liu et al., 1997] after which the buffer was exchanged through dialysis with a 10 kDa cutoff against pyrogen-free PBS containing 20% glycerol. The protein was then filtered through a Posidyne membrane (0.2 μm, Pall Gelman Laboratory, Ann Arbor, MI). The concentration of LPS in the final AIMP1 preparation was below 20 pg/mg, as determined with a Limulus Amebocyte Lysate QCL-1000 kit (BioWhittaker). In parallel, 10 ml of PBS-20% glycerol underwent the same protocol used for LPS extraction from recombinant AIMP1 (rAIMP1) to be used as the vehicle for control samples in all experiments.

AIMP1 STABILITY IN CELL CULTURE MEDIUM

Recombinant AIMP1, at a concentration of 250 nM, was incubated at 37°C in conditioned Ham's F-12 medium supplied with 10% FBS. The cultured medium used was taken from a PAEC plate that had been kept in culture for 48 h. At defined time points 30 μl samples were collected and loaded on SDS–PAGE for Western blot analysis.

CIRCULAR DICHROISM SPECTROMETRY

Circular dichroism spectra were recorded for rAIMP1 protein (0.1 mg/ml) at temperatures between 20 and 90°C on a JASCO J-815 spectometer equipped with a Peltier temperature controller, using a 1-cm path length quartz cuvette. Spectra were recorded between the wavelengths of 195 and 250 nm with a 1.0-nm step size and slit bandwidth of 1.0 nm. Signal averaging time was 8 s and ellipticities were reported as mean residue ellipticity in $deg.cm^2/dmol$. Spectra recorded for the vehicle were subtracted from rAIMP1 spectra.

WESTERN BLOT ANALYSIS

Protein samples were loaded on SDS–PAGE, transferred to nitrocellulose membrane and blocked with 5% non-fat milk powder in TBS containing 0.1% Tween 20 (TBST). The membrane was incubated with specific primary antibody diluted in TBST-1% milk O.N. at 4°C; the appropriate HRP-conjugated secondary antibody was diluted 1:10,000 in TBST-1% milk for 1 h at room temperature and membrane developed using ECL Western blotting substrate kit (Thermo Fisher Scientific, Rockford, IL).

CELL ADHESION ASSAY

Cell adhesion assay was performed using fibronectin (FN) pre-coated 96-well plates (Becton Dickinson, Franklin Lakes, NJ). Cells were serum-starved for 16 h, detached with 5 mM EDTA, supplied with Ham's F-12 medium containing 1% FBS and 100 nM rAIMP1 or vehicle and plated (5×10^4 cells/well) on FN pre-coated plates. After 20 min, cells were fixed with paraformaldehyde (PFA) 4% in PBS, stained with 50 μl crystal violet solution (0.5% crystal violet, 20% methanol) for 10 min at room temperature and stain was solubilized with 100 μl Sorenson's buffer (0.1 M sodium citrate, 50% ethanol, pH 4.2). After solubilization the optical density of each well was measured with a multimode microplate reader (Infinite 200, Tecan) at 595 nm. Triplicate wells and blank well without cells were run for each treatment.

CELL VIABILITY ASSAY

AIMP1 role in inhibiting cell viability was monitored by measuring the cellular conversion of a tetrazolium salt into a formazan product detected using a 96-well plate reader (CellTiter 96 Non-Radioactive Cell Proliferation Assay; Promega, Madison, WI). Cells were serum-starved for 16 h, then plated on 96-well dishes (1×10^4 cells/well), treated with rAIMP1 or vehicle in presence of 10% FBS and cultivated for 24 h. After treatment, 15 μl of Dye Solution (containing the tetrazolium component) were added and cells incubated for 4 h before adding the Stop Solution to solubilize the formazan product. After an incubation of 1 h, the absorbance at 570 nm was recorded using a 96-well plate reader (Tecan, Infinite 200).

The role of α5β1 integrin in AIMP1 inhibitory effect on EC survival was monitored by measuring the cellular conversion of a tetrazolium salt into a formazan product detected using a 96-well plate reader (CellTiter 96 Non-Radioactive MTT Assay; Promega). Cells were starved for 16 h in serum-free medium, detached with 5 mM EDTA and 7×10^4 cells were incubated with 800 nM anti-α5β1 integrin antibody or control for 15 min at 4°C before plating. Recombinant AIMP1 (100 nM) or vehicle were added in presence of 10% FBS, cells were plated in triplicate at a density of 2×10^4 cells/well and cultivated for 24 h. MTT assay was performed after 24 h as described above.

Absorbances were normalized to vehicle and expressed as values relative to positive control.

FLOW CYTOMETRY

Cells were serum-starved for 16 h, then plated on 24-well dishes (1×10^5 cells/well), treated with rAIMP1 or vehicle in presence of 10% FBS and cultivated for 4, 8, and 24 h. After treatment, the cells were detached with 0.25% trypsin, washed twice in cold PBS-5% FBS and resuspended in cold PBS-5% FBS at a concentration of 1×10^6 cells/ml. Apoptotic cells were determined by staining with propidium iodide and annexin V (FITC Annexin V Apoptosis Detection Kit; Becton-Dickinson) using a flow cytometer (FACS Calibur). Analysis was performed with Cell Quest software.

IMMUNOFLUORESCENCE ANALYSIS

Indirect immunofluorescence analysis was performed on time course experiments of PAEC stimulation with rAIMP1 to study the subcellular localization of the exogenous protein. PAEC, maintained in their growth medium, were plated (1×10^4 cells/well) in 24-well plates onto glasses covered with 1% porcine gelatine (coating layered O.N. at 4°C). Cells were cultured for 30 h, serum starved for 16 h and treated with 50 nM rAIMP1 in 500 μl of 10% FBS containing culture medium.

After stimulation, cells were fixed in 4% PFA, permeabilized in PBS-0.1% Triton X-100 and blocked in PBS-1% BSA-5% goat serum. Cells were then incubated with primary antibodies followed by Alexa Fluor 488- or Alexa Fluor 568-conjugated secondary antibodies (Invitrogen, Carlsbad, CA). Moreover, cells were stained for 30 min with propidium iodide to decorate nuclei or for 20 min with phalloidin to stain the cytoskeleton. Fluorescence was examined with a Leica confocal microscope at a 63× magnification (Leica TCS SPE). For confocal analysis, optical sections were recorded at 0.5 μm intervals throughout the cells. Pictures were handled with Leica LAS and Adobe Photoshop software.

CELL TREATMENT, PROTEIN EXTRACTION, AND SAMPLE PREPARATION FOR 2-D ELECTROPHORESIS

For phosphoproteomic analysis, cells were serum starved for 16 h and treated with 200 nM AIMP1 or vehicle in Ham's F-12 without FBS for 10 and 30 min. Four biological replicates were performed for each treatment. After treatment, cells were washed twice with PBS and twice in sucrose buffer (250 mM sucrose, 10 mM Tris–HCl, pH 7). Protein extraction was performed following the protocol from Yan et al. [2007]. Cell samples were lysed in solubilization buffer (40 mM Tris, 7 M urea, 2 M thiourea, 4% 3-[(3-cholamidopropyl)dimethylammonio]-1-propanesulfonate (CHAPS), 65 mM dithiothereitol (DTT), 1 mM ethylenediamine-tetra-acetic acid, 1× protease inhibitor cocktail, 0.1 g/l RNase A, and 0.1 g/l DNase) and sonicated (5 s/cycle, three cycles; 0°C). After centrifugation at 13,000 × *g* for 30 min at 4°C, the supernatant was collected as the protein sample. Before subsequent analysis, the sample was concentrated and desalted using the Ultrafree-0.5 Centrifugal Filter Device (Millipore) according to manufacturer's protocol. Protein concentration was determined using Bradford protein assay kit (BioRad, Marnes-la-Coquette, France).

2-D ELECTROPHORESIS

2-D electrophoresis (2-DE) was performed according to Jacobs et al. [2001], with some modifications. Isoelectrofocusing of proteins was performed at 20°C in 18 cm IPG 4-7 strips (GE Healthcare), using the Ettan IPGphor system (GE Healthcare). Prior to SDS–PAGE, the IPG strips were equilibrated twice for 15 min in a buffer containing 50 mM Tris–HCl pH 8.8, 6 M urea, 30% glycerol, 2% SDS, plus 1% DTT for the first equilibration step, 2.5% iodoacetamide, and traces of bromophenol blue for the second one. SDS–PAGE was performed on 12.5% polyacrylamide gels according to Laemmli [Laemmli, 1970] but without stacking gel, in a PerfectBlue Dual gel System, 20 × 20 cm (PeQLab). The run was carried out at 60 mA/gel at 16°C until the tracking dye front reached the bottom of the gel. Each treated sample was run simultaneously to its control.

In order to visualize phosphorylated proteins, gels were stained with Pro-Q Diamond (Molecular Probes Inc, Eugene, OR) following the protocol of Agrawal and Thelen [2005]. After image acquisition, gels were stained for total protein with SYPRO Ruby protein gel stain (Molecular Probes) according to the manufacturer's protocol.

Images were acquired by CCD camera (ProXPRESS 2-D Perkin Elmer) with the following parameters: excitation 540/25 and emission 590/35 nm for phosphoprotein staining, and excitation 460/80, emission 650/150 for Sypro staining, respectively. Before MS analysis, the gels were stained in Coomassie Blue R350 [Marchetti-Deschmann et al., 2009].

IMAGE ANALYSIS

Image analysis was performed by the ImageMaster 2D Platinum 5.0 software package (GE Healthcare). Spot detection and gel matching were carried out automatically and checked manually. The volume of each spot was normalized to the total volume of spots in the gel (vol%). Analysis was performed in order to identify spots with

qualitative (presence/absence) and quantitative ($\geq$1.5-fold) spot volume increase/decrease between treatment and control. Spots that fulfilled these criteria in at least three experiments were considered significant and underwent mass spectrometry analysis. For ProQ Diamond stained gels all spots were also required to be detected and matched in SYPRO Ruby image counterpart.

Quantitative differences were calculated for both SYPRO Ruby and ProQ Diamond images. Proteins found as having differential spot volumes by ProQ Diamond staining were considered as differentially phosphorylated only if they did not also show a significant variation by SYPRO Ruby staining.

PROTEIN IDENTIFICATION BY MASS SPECTROMETRY (MS)

Protein spots or bands were excised from gels and, after trypsin digestion, were analyzed by a HP 1100 nanoLC system coupled to a XCT-Plus nanospray-ion trap mass spectrometer (Agilent), as described in Mila et al. [2009]. Mass spectrometry data were fed to the Mascot search algorithm for searching against the NCBI non-redundant database number 20100402 (http://www.matrixscience.-com). Hits with a probability-based MOWSE score higher than 47 were considered significant ($P < 0.05$). Since the protein database for *Sus scrofa* is not complete, when a protein was not present as porcine in the database, we accepted its identification from *Bos taurus* or *Homo sapiens*.

SUBCELLULAR FRACTIONATION

PAEC were serum starved for 16 h and subcellular fractionation was performed according to Kim et al. [1999] with some modifications. All procedures were done at 4°C. PAEC from one 150-mm culture dish (8×10^6 cells) were resuspended in 1 ml of buffer A (25 mM Tris pH 7.4, 1 mM EDTA, 0.5 mM EGTA, 10 mM NaCl, 0.5 mM PMSF, 1× protease inhibitor cocktail), put through three freezing and thawing cycles in liquid nitrogen and homogenized 40 times with a tight Dounce homogenizer (Kontes Glass, Vineland, NJ). A one-tenth volume buffer A containing 2.5 M sucrose was added to the homogenate. The homogenate was centrifuged at $1{,}000 \times g$ for 10 min (step A). The supernatant of step A was centrifuged at $100{,}000 \times g$ for 1 h (step B). The pellet of step B was resuspended in PBS-1% NP40 (containing 1× protease inhibitor cocktail and 0.5 mM PMSF) and stored as the membrane fraction; the supernatant of step B was stored as the cytosolic fraction.

AFFINITY PRECIPITATION AND PURIFICATION OF AIMP1-BINDING MOLECULES

The subcellular fractions were dialyzed for 16 h at 4°C against PBS containing 1× protease inhibitor cocktail, then incubated with rAIMP1 or vehicle for 2 h at 4°C; rAIMP1 was then precipitated using nickel affinity interaction (Ni Sepharose high performance; GE Healthcare) for 1 h at 4°C.

After incubation, the resin was spinned down, washed with washing buffer (50 mM Na_2HPO_4, 200 mM NaCl, 0.1% NP40, 2 mM EDTA, 2 mM Na_3VO_4, 1 mM PMSF, 1× protease inhibitor cocktail), and resuspended in 30 μl loading buffer (62.5 mM Tris–HCl pH 6.8, 20% glycerol, 2% SDS, 5% β-mercaptoethanol, 0.025% bromo-phenol blue). Samples were resolved on SDS–PAGE and stained with Coomassie Brilliant Blue; the differential bands were excised and identified by mass spectrometry analysis.

PULL-DOWN ASSAY

Subcellular fractions were dialyzed for 8 h against PBS containing 1× protease inhibitor cocktail at 4°C and were then incubated with rAIMP1 or vehicle for 16 h at 4°C. Ni-Sepharose high performance beads were added to the cellular fractions and incubated for 1 h at 4°C. The samples were then centrifuged and the supernatant was removed. The beads were washed with washing buffer (50 mM Na_2HPO_4, 200 mM NaCl, 0.1% NP40, 2 mM EDTA, 2 mM Na_3VO_4, 1 mM PMSF, 1× protease inhibitor cocktail) and resuspended in 200 μl loading buffer. 20 μl of sample were loaded on SDS–PAGE and the putative rAIMP1-binding proteins were identified through Western blot analysis.

CO-IMMUNOPRECIPITATION

Subcellular fractions were dialyzed for 8 h against PBS containing 1× protease inhibitor cocktail at 4°C, incubated with rAIMP1 for 16 h at 4°C and mixed, for 30 min at 4°C, with anti-filamin-A, anti-α-tubulin, anti-vinculin, anti-cingulin, or control antibodies, pre-coupled with protein A or G Sepharose beads. The samples were then centrifuged and the supernatants removed. Beads were washed with PBS-0.1% NP40 and resuspended in 20 μl loading buffer. Samples were then loaded on SDS–PAGE and immunoblotted with anti-His-probe antibody to recognize rAIMP1.

RESULTS

AIMP1 CONFORMATION AND STABILITY

The stability of AIMP1 in conditioned medium was verified. AIMP1 (250 nM) was incubated at 37°C in conditioned Ham's F-12 medium supplied with 10% FBS. At defined time points, 30 μl samples were collected for SDS–PAGE and Western blot analysis. A high amount of undegraded AIMP1 was still present after 54 h of incubation (Fig. 1A). In order to obtain information on the secondary and tertiary structure of AIMP1, circular dichroism (CD) experiments were performed using a JASCO spectrometer. CD can be used to study how the structure of a molecule changes as a function of temperature. The AIMP1 circular dichroic spectrum was recorded between 195 and 250 nm at temperatures ranging from 20 to 99°C. A change in signal was seen when temperature increased, suggesting a progressive loss of the molecule's 3-D organization (Fig. 1B). Plotting the mean residue ellipticity of AIMP1 against temperature, a steep change in CD signal occurs around 50–70°C, suggesting that denaturation of the protein occurs at temperatures above 50°C (Fig. 1C).

AIMP1 INHIBITS CELL ADHESION

On the basis of the literature data describing EMAP II inhibitory effect on MEC adhesion through a direct interaction between EMAP II and α5β1 integrin [Schwarz et al., 2005], the hypothesis of an inhibitory effect elicited by AIMP1 on PAEC adhesion was investigated. To do this, a cell adhesion assay was performed: cells were supplied with Ham's F-12 medium containing 1% FBS and 100 nM AIMP1 or vehicle, plated on FN pre-coated plates and left to

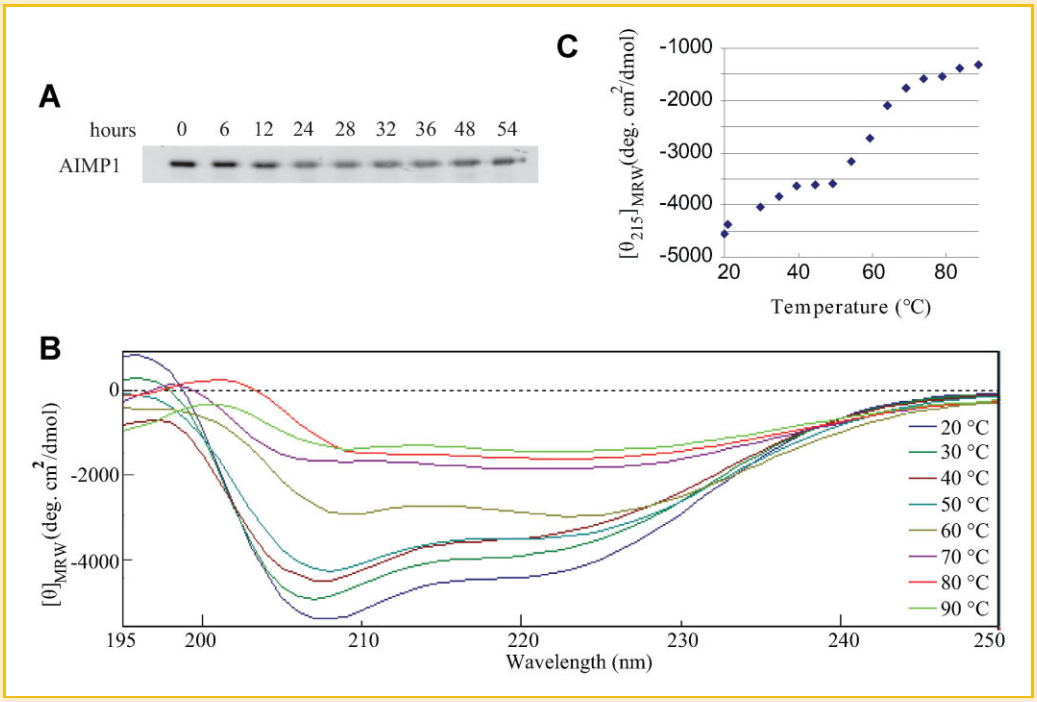

Fig. 1. A: AIMP1 stability in conditioned medium. Recombinant AIMP1 (250 nM) was incubated with conditioned Ham's F-12 supplied with 10% FBS at 37°C for the indicated times. The protein was immunoblotted using anti-EMAP II antibody recognizing AIMP1. B: Thermal denaturation of AIMP1. Circular dichroism spectra were recorded for AIMP1 (0.1 mg/ml) between 195 and 250 nm during heating from 20 to 90°C and reported as mean residue ellipticity (θ_{MRW}). Data were plotted for each 10°C interval as indicated in figure. C: Thermal denaturation of AIMP1 shows a steep change in CD signal around 50–70°C. Mean residue ellipticity (deg.cm^2/dmol) at 215 nm was plotted against temperature.

adhere for 20 min. Measurement of absorbance values after crystal violet staining showed that AIMP1 inhibits cell adhesion on FN (Fig. 2A).

An inhibitory effect on EC adhesion on FN had already been proposed for EMAP II [Schwarz et al., 2005]. In this work also AIMP1 was demonstrated to impair EC adhesion.

Since EC adhesion to FN can be mediated by α5β1 integrin, it is possible that this receptor has a role in AIMP1 ability to interfere with cell adhesion as is the case for EMAP II [Schwarz et al., 2005].

AIMP1 INHIBITORY EFFECT ON PAEC VIABILITY IS REVERTED BY PRE-TREATMENT WITH ANTI-α5β1 INTEGRIN ANTIBODY

Since an appropriate cell adhesion is necessary for cell survival and proliferation, the role of α5β1 integrin in the effect elicited by AIMP1 on EC survival was investigated. It is known from literature that AIMP1 inhibits EC survival [Park et al., 2002c]. A viability assay was performed to confirm AIMP1 inhibitory activity on EC survival. Results showed that AIMP1 inhibits PAEC viability starting from a concentration of 100 nM (Fig. 2B). It was then investigated whether α5β1 integrin has a role in the inhibitory effect of AIMP1 on PAEC survival. Indeed, pre-treatment of PAEC with anti-α5β1 integrin antibody is able to revert AIMP1 inhibitory effect on PAEC viability (Fig. 2C). This result shows the involvement of α5β1 integrin in AIMP1 activity on ECs. On the basis of literature data and the results obtained in this study from the biological assays, it could be hypothesized that the impairment of cell adhesion could be one of the mechanism through which AIMP1 interferes with EC survival. Indeed, cells stimulated with AIMP1 during the adhesion process, as in the viability assays, show increased apoptosis with respect to control samples after 24 h (Fig. 2D).

AIMP1 ACTIVATES ERK AND JNK IN PAEC

In biological assays, AIMP1 showed an inhibitory activity on EC viability and on endothelial cell adhesion. Western blot analysis was performed to identify some of the signaling molecules activated upon PAEC stimulation with AIMP1. On the basis of the experimental results which show that AIMP1 activity on PAEC could be mediated by a membrane receptor (α5β1 integrin), the possible phosphorylation of two major mitogen-activated protein kinases (MAPKs) was investigated: JNK, which is involved in apoptosis, cell differentiation and proliferation and ERK, involved in functions including the regulation of meiosis, mitosis, post-mitotic functions in differentiated cells and in a great variety of signaling transduction pathways activated by extra-cellular molecules. Cells were treated with AIMP1 in time course experiments, with six time points from 0 to 180 min. Results show that AIMP1 induces ERK and JNK activation through phosphorylation after 10-min treatment of PAEC (Fig. 3).

LOCALIZATION OF EXOGENOUS AIMP1 AFTER TREATMENT OF ENDOTHELIAL CELLS

In order to analyze AIMP1 subcellular localization, immunofluorescence experiments were performed. PAEC were treated with 50 nM AIMP1 in time course experiments from 15 min to 6 h. Exogenous

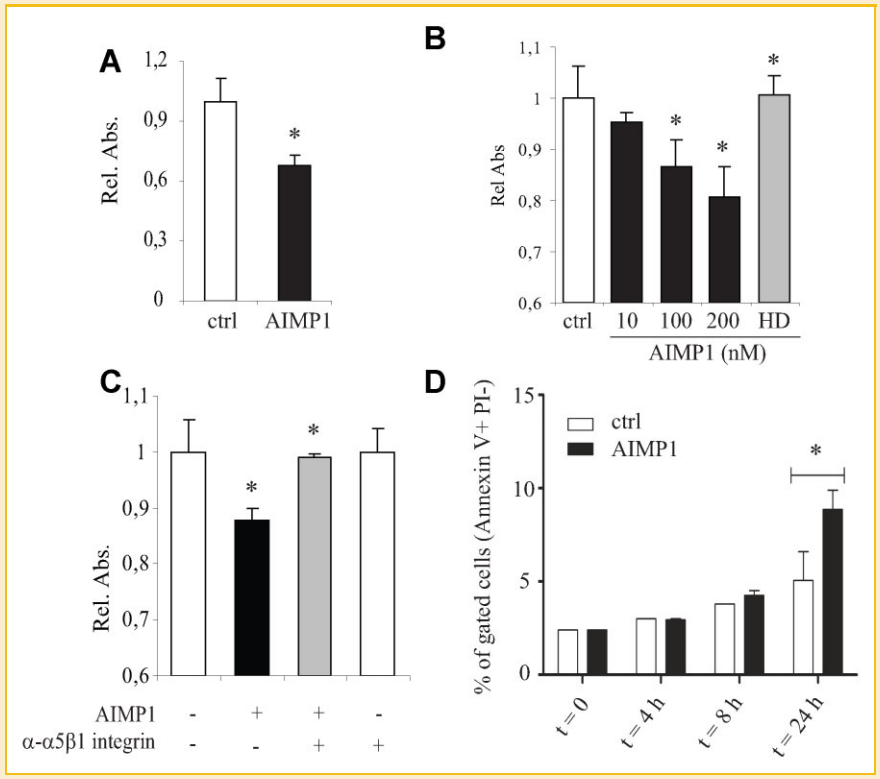

Fig. 2. Biological assays. A: AIMP1 inhibits PAEC adhesion on fibronectin. Cells were incubated with 100 nM AIMP1 or vehicle in Ham's F-12 medium supplied with 1% FBS and plated on fibronectin pre-coated plates. Data represent mean ± SD. *Statistically significant difference compared with control ($P < 0.05$). Graphics report relative absorbance values normalized to vehicle (ctrl). B: AIMP1 inhibits PAEC viability. Cells were cultured in Ham's F-12 medium supplied with 10% FBS in presence of indicated stimuli. After 24 h, MTT assay was performed. HD indicates the heat-denaturated protein incubated at 99°C for 30 min before stimulation and used at a concentration of 200 nM. Data represent mean ± SD. *Statistically significant difference compared with control ($P < 0.005$). C: Pre-treatment of cells with anti-α5β1 integrin antibody reverts AIMP1 inhibitory effect on cell viability. Cells were incubated with anti-α5β1 integrin antibody (0.8 μM) before treatment with AIMP1 (100 nM). Treatment with anti-α5β1 integrin antibody alone shows no difference with respect to the control. Data represent mean ± SD. *Statistically significant difference compared with control ($P < 0.005$). D: AIMP1 induces PAEC apoptosis after 24 h. Cells were plated in Ham's F-12 medium supplied with 10% FBS in presence of 100 nM AIMP1 or vehicle. The percentage of apoptotic cells was determined by staining with propidium iodide and annexin V. *Statistically significant ($P < 0.05$ two-way ANOVA followed by Bonferroni's test).

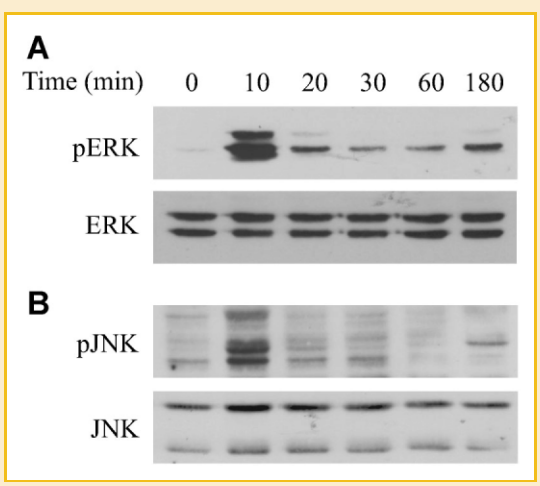

Fig. 3. AIMP1 activates ERK and JNK after a 10-min treatment. Cells were treated with 200 nM AIMP1 in a time course experiment. Membranes were blotted with anti-pERK (A) or anti-pJNK (B) antibodies and normalized to the respective total ERK and JNK proteins.

AIMP1 was previously demonstrated to be internalized almost immediately after cellular incubation [Yi et al., 2005] and this datum was confirmed in this work using an immunofluorescence technique. As soon as 30 min after AIMP1 treatment, the exogenous protein enters the cell but does not enter the nucleus, as verified by confocal microscope analysis in cells treated with AIMP1 up to 6 h (data not shown). AIMP1 localization inside the cell or on the cell membrane does not occur when the protein is heat inactivated for 30 min at 99°C before stimulation (Fig. 4A,B). Interestingly, AIMP1 distribution often appears to be asymmetric (Fig. 4C,D) and, furthermore, AIMP1 localizes at the level of cell protrusions (Fig. 4C).

IDENTIFICATION OF AIMP1-BINDING MOLECULES

To understand exogenous AIMP1 activity on ECs it is important to identify the molecules able to interact with it. To identify AIMP1-binding proteins, the cytosolic and membrane fractions from PAEC lysates were used. Since it was shown that starvation increases EMAP II binding to the cell surface [Chang et al., 2002] serum starvation was used as an experimental condition to isolate AIMP1-binding proteins. AIMP1-binding proteins from the subcellular

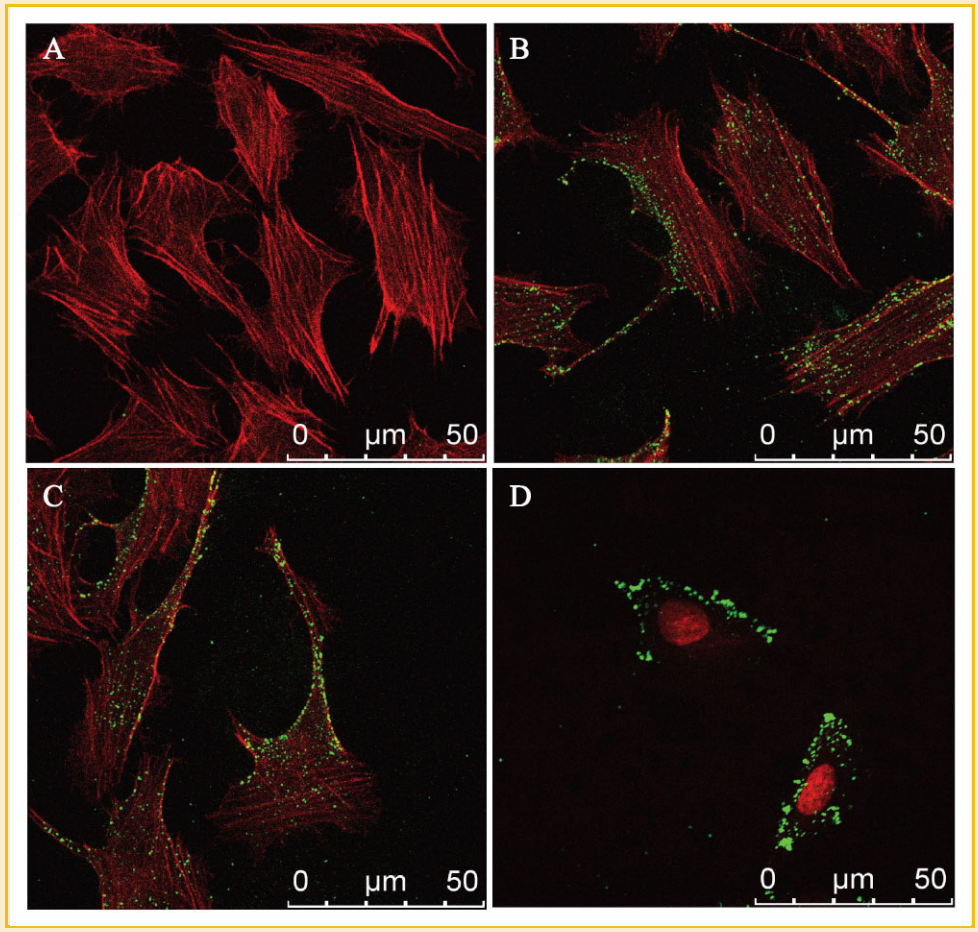

Fig. 4. Subcellular localization of exogenous AIMP1. A: Control: 1 h heat-denaturated AIMP1 (HD AIMP1) treated cells. B: 1 h AIMP1-treated cells. C: AIMP1 concentrates in the cell protrusions. Actin is stained in red (phalloidin) and AIMP1 in green (anti-myc antibody). D: Exogenous AIMP1 distribution in the cell is asymmetric. Nucleus is stained in red (PI) and AIMP1 in green (anti-myc antibody).

fractions were precipitated with Ni-Sepharose beads and the precipitates were loaded on SDS–PAGE (Fig. 5A). Identification of differential bands between AIMP1 samples and control samples was performed by nanoliquid chromatography–nanospray–ion trap mass spectrometry (LC–MS/MS).

Table I shows 10 of the putative AIMP1-interacting proteins identified in the membrane and cytosolic fractions. Other proteins were found, including glycyl-tRNA synthetase and coatomer subunit beta protein (β-cop, data not shown), the interaction of which with AIMP1 has already been described [Park et al., 2005a; Han et al., 2007]. Interestingly, six of the identified proteins were cytoskeletal or cytoskeleton-associated proteins which are involved in cellular architecture maintenance and remodeling.

From the set of AIMP1-interacting proteins obtained from the affinity purification we decided to focus on the cytoskeletal or cytoskeleton-associated proteins. The results were validated through pull-down and co-immunoprecipitation assays and confirmed interaction with filamin-A, α-tubulin, vinculin, and cingulin (Fig. 5B,C). These results suggest a possible involvement of proteins controling adhesion and cytoskeletal remodeling in the signaling pathway activated by exogenous AIMP1 in PAEC.

AIMP1 CO-LOCALIZES WITH CINGULIN AND FILAMIN-A IN ENDOTHELIAL CELLS

To see whether AIMP1 co-localized in the cell or at the cell membrane with the AIMP1-interacting proteins previously identified or with α5β1 integrin, immunofluorescence double-staining experiments were performed. After 1 h treatment of subconfluent PAEC with 100 nM AIMP1, partial co-localization was observed between AIMP1 and cingulin as well as between AIMP1 and filamin-A (Fig. 6) but no co-localization was observed between AIMP1 and vinculin, α-tubulin or α5β1 integrin (data not shown).

AIMP1 TREATMENT OF ENDOTHELIAL CELLS INDUCES α-TUBULIN PHOSPHORYLATION

To further investigate the signaling pathways activated by exogenous AIMP1 in PAEC, the phosphorylation events following AIMP1 treatment were investigated through a 2-DE phosphoproteomic approach. This technique provides an overview of the entire phosphoproteome in definite experimental conditions. PAEC were treated with 200 nM AIMP1 or vehicle for 10 and 30 min. About 1,200 protein spots were detected by the SYPRO Ruby stain and about 120 spots were visualized by a phosphoprotein-specific stain.

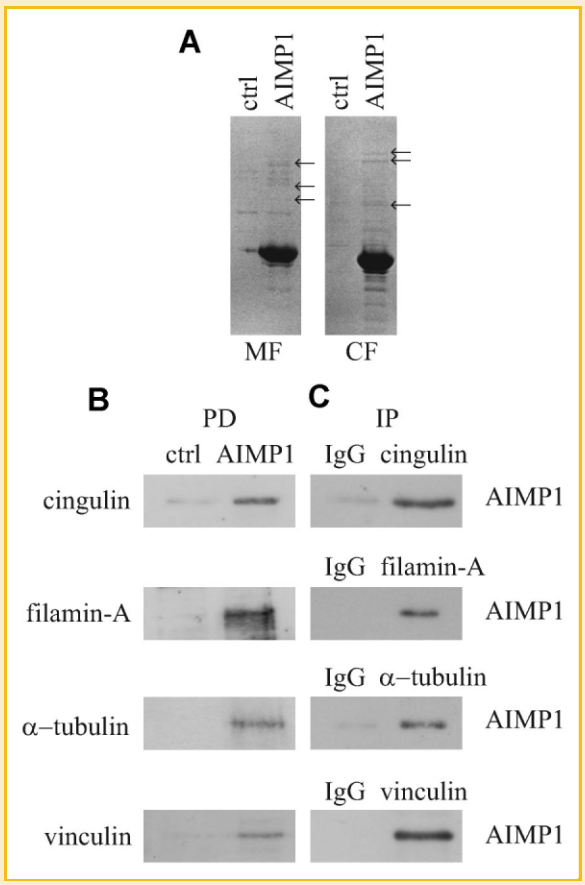

Fig. 5. Identification of AIMP1-interacting proteins. A: Affinity purification of AIMP1-interacting proteins. SDS–PAGE stained in Coomassie Brilliant Blue of two representative experiments performed with the membrane fraction (MF) or with the cytosolic fraction (CF); the black arrows indicate the differential bands between AIMP1-functionalized resin and control (ctrl), functionalized with vehicle, obtained in these two representative experiments. Differential bands were excised and proteins identified by mass-spectrometry analysis. B: Pull-down assay. Subcellular fractions (membrane fraction or cytosolic fraction) were incubated with AIMP1 or vehicle and precipitated by nickel affinity. Cingulin, filamin-A, α-tubulin, and vinculin were immunoblotted with the respective antibodies. C: Subcellular fractions were incubated with AIMP1 and immunoprecipitated with anticingulin, anti-filamin-A, anti-α-tubulin, and anti-vinculin antibodies, or control IgG. Precipitated proteins were immunoblotted with anti-His-probe antibody recognizing recombinant AIMP1.

From each class (AIMP1 10 min, control 10 min, AIMP1 30 min, and control 30 min) a set of four gels was stained with ProQDiamond followed by Sypro Ruby, imaged and analyzed as described in the Materials and Methods section. The spots which significantly varied among treated samples and controls were excised and identified by LC-MS/MS. For both time points, no qualitative differences were highlighted. No significant spots were identified following 30-min treatment. The proteins which were differentially phosphorylated between treated cells and controls upon 10-min treatment are α-tubulin, elongation factor 1δ and 60S acidic ribosomal protein P2 (indicated in Table II and Fig. 7). Among these differentially phosphorylated proteins was α-tubulin, the phosphorylation of which is twofold up-regulated in treated samples compared to the controls (Fig. 7 and Table II).

DISCUSSION

Despite its role as a cofactor of the ARS complex [Quevillon et al., 1997; Park et al. 1999; Kim et al., 2000b; Shalak et al., 2001], AIMP1, when secreted, also acts as a cytokine on different cell types [Ko et al., 2001; Park et al., 2002a,c, 2005b; Chang et al., 2002]. AIMP1 has shown to be a cytokine activating immune cells and ECs since it is highly secreted from Raw 264.7 cells stimulated by TNF [Park et al., 2005b]. AIMP1 has higher cytokine activity on immune and ECs than its cleaved C-terminal domain, EMAP II [Park et al., 2002c; Yi et al., 2005] which was initially thought to be the effective cytokine [Kao et al., 1994a,b; Knies et al., 1998; Shalak et al., 2001].

Although the administration of both recombinant EMAP II and AIMP1 has been shown to inhibit tumor growth by inhibition of angiogenesis [Schwarz et al., 1999; Lee et al., 2006], the mechanism surrounding their angiostatic effect is poorly understood. Angiogenesis, the growth of new blood vessels, is essential for pathological processes such as tumor growth and metastasis [Carmeliet, 2005] and ECs play a key role in all aspects of this cellular event [Jain, 2003]. In this work, we have analyzed the signaling pathways activated by exogenous AIMP1 on endothelial cells (PAEC) using a wide range of in vitro techniques.

EMAP II has also been shown to inhibit microvascular endothelial cell (MEC) adhesion to FN and to delay cell spreading through a direct interaction with α5β1 integrin [Schwarz et al., 2005]. Furthermore, EMAP II was shown to disassemble the cytoskeletal

TABLE I. AIMP1-Interacting Proteins Obtained by Affinity Purification

Fraction	LC-MS/MS identification	Accession number	Peptide number	Seq. cov. (%)	Score
CF	Filamin-A	gi116241365	34	32	1791
	GRP78	gi14916993	23	28	1058
	Vimentin	gi76097691	13	41	695
	α-Tubulin	gi81174755	4	11	313
	Glycogen phosphorylase	gi106073338	6	7	213
MF	Cingulin	gi194036221	4	3	67
	Vinculin	gi50403675	3	3	59
	Ras GTPase-activating-like protein (IQGAP3)	gi229462887	2	2	59
	Protocadherin-11 X-linked	gi75071591	2	2	57
	Rho GTPase-activating protein 29 (ARHGAP29)	gi194036908	2	2	52

First column indicates the subcellular fraction in which the protein was found, second and third columns report the name of the identified protein and its gi accession number; the table also shows the number of peptides recognized by the Mascot algorithm and the percentage of sequence coverage; hits with a probability-based MOWSE score higher than 47 were considered significant ($P < 0.05$).

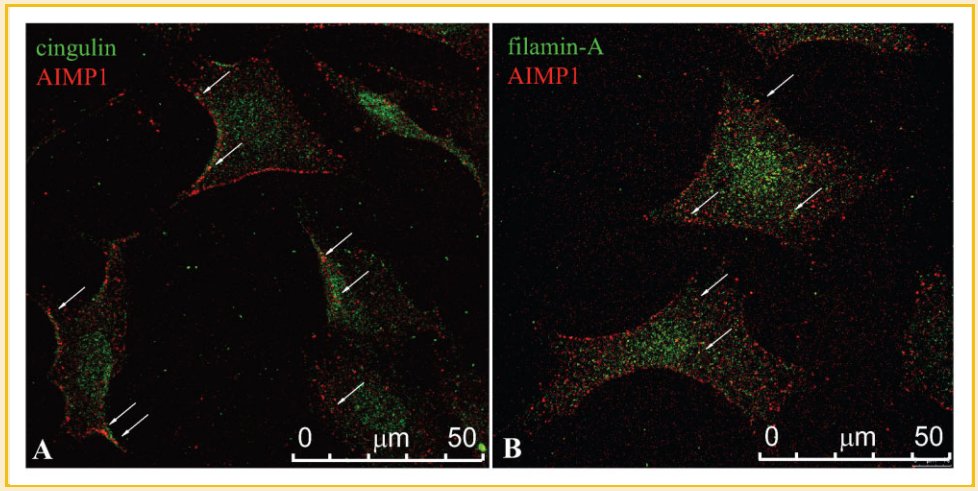

Fig. 6. AIMP1 co-localizes with cingulin and filamin-A in the cells. A: Merge between anti-cingulin (green) and anti-myc (red) staining. B: Merge between anti-filamin-A (green) and anti-myc (red) staining. The co-localization positions are indicated by the arrows. Cells were treated with 100 nM AIMP1 for 1 h, then fixed and stained.

TABLE II. Phosphorylated Proteins Upon 10 Min AIMP1 Treatment of PAEC

Spot no.	Change-fold	LC–MS/MS identification	Accession number	Peptide number	Seq. cov. (%)	Apparent pI/MW (kDa)	Theoretical pI/MW (kDa)	Mascot score
496	↑ 1.8	α-Tubulin	gi81174755	18	42	~5/~50	4.86/50	589
482	↑ 2.6	Elongation factor 1δ	gi172047287	15	32	~5/~30	4.94/30	564
643	↑ 2.1	60S acidic ribosomal protein P2	gi3914781	4	21	~4.5/~12	4.42/11.6	218

The spot number corresponding to each identified protein is indicated in the first column. Change fold values indicate the mean obtained from at least three experiments (↑: up-regulated in AIMP1 samples). Name of identified protein and gi accession number are shown in the third and fourth columns. The table also shows the number of peptides recognized by the Mascot algorithm and the percentage of sequence coverage; hits with a probability-based MOWSE score higher than 47 were considered significant ($P < 0.05$). Apparent pI and MW are obtained from the 2-DE gel, theoretical pI and MW are obtained from Mascot database.

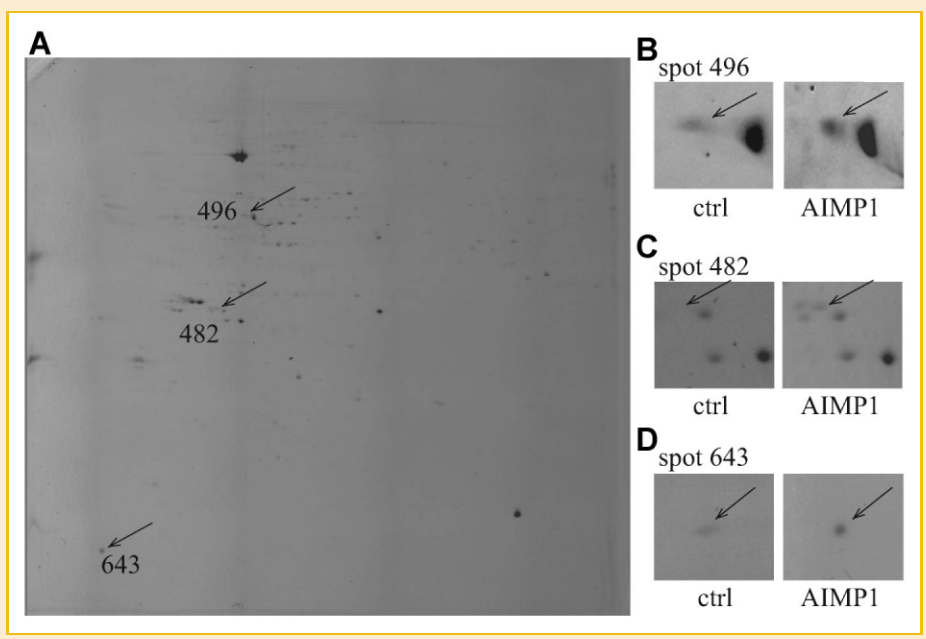

Fig. 7. The phosphorylation of α-tubulin, elongation factor 1δ and 60S acidic ribosomal protein P2 is up-regulated upon 10-min AIMP1 treatment of PAEC. Cells were treated with 200 nM AIMP1. A. ProQ Diamond stained gel of a representative experiment. Spots that showed a significant change in volume percentage are indicated by the arrows and identified by the spot number. B–D: Single spot magnifications of ProQ Diamond stained gels from control and treated samples (indicated by the arrow).

architecture of actin fiber networks and FN matrix assembly [Schwarz et al., 2005]. Evidence has been provided to show that α5β1 integrin and its ligand FN are coordinately up-regulated in blood vessels in human tumor biopsies and play critical roles in angiogenesis, resulting in tumor growth in vivo. Three classes of α5β1 integrin antagonists (antibody, peptide, and a new non-peptide antagonist) have been shown to block growth factor-stimulated angiogenesis [Kim et al., 2000a]. These results implicate that integrin is the receptor for FN during angiogenesis [Kim et al., 2000a] and may be an important target for EMAP II anti-angiogenic function [Schwarz et al., 2005].

In this study, it was demonstrated that AIMP1 inhibits PAEC adhesion on FN coating. We also confirmed that AIMP1 inhibits PAEC viability and showed that α5β1 integrin is also involved in the inhibitory effect elicited by AIMP1 on PAEC survival: this was supported by the observation that, when blocking α5β1 integrin with the specific antibody, AIMP1 effect on PAEC viability was reverted. Furthermore, AIMP1-induced apoptosis is at least partially responsible for reduced viability of AIMP1-stimulated PAEC. Our hypothesis is that cell adhesion impairment could be one of the mechanisms through which AIMP1 interferes with EC survival.

To shed light on the mechanisms leading to these results, the signaling pathways activated by exogenous AIMP1 in ECs were investigated. We observed that stimulation with 200 nM AIMP1 activates both ERK and JNK in PAEC. Activation of these two kinases following AIMP1 treatment of ECs has already been described [Park et al., 2002c]. In particular, ERK was shown by the authors to be activated in BAEC treated with 1 nM AIMP1, resulting in induction and activation of MMP9 and in induction of EC migration, while JNK activation was obtained with concentrations from 10 to 100 nM and mediated EC death [Park et al., 2002c]. Since ERK and JNK activation has been observed upon FN-induced α5β1 integrin stimulation in other cell models [Mendes et al., 2010; Sen et al., 2010], it would be interesting to investigate in the future both whether α5β1 integrin is involved in the induction of cell migration and ERK-dependent MMP9 expression as well as whether JNK is involved in the transduction of AIMP1 effects on cell adhesion and survival.

Immunofluorescence experiments performed on AIMP1-treated PAEC showed that exogenous AIMP1 distributes in the cells with an asymmetric pattern and that it concentrates in the cell protrusions. Observation of the peculiar distribution pattern of AIMP1 when administered to cells and co-localization with two important cytoskeleton-related proteins (filamin and cingulin) led us to speculate that AIMP1 might affect cellular architecture maintenance and remodeling. The ability of EMAP II to interfere with cell cytoskeleton organization has already been described. Keezer et al. [2003] demonstrated that, in adherent ECs, EMAP II stimulation caused an increase of intracellular actin fibers and focal adhesion. On the other hand, Schwarz et al. [2005] have demonstrated that microvascular ECs exposed to EMAP II during the adhesion process undergo rapid disassembly of the actin stress fiber network. These results highlight two contexts in which EMAP II interferes with cell cytoskeleton organization.

Results obtained by "fishing" new AIMP1 interactors strengthen the hypothesis of the role of AIMP1 in modifying cell structure by controling adhesion and cytoskeletal remodeling. In particular, four cytoskeletal or cytoskeleton-associated proteins interacting with AIMP1 have been discovered: vinculin, cingulin, α-tubulin, and filamin-A.

Among these, vinculin is localized at the cell membrane in cell–cell junctions and cell–substrate junctions [Sechi and Wehland, 2000] and cingulin is localized at tight junctions in confluent cells [Guillemot et al., 2004] while diffusely distributed within the cytoplasm in subconfluent cells [Stevenson et al., 1989]; α/β tubulin heterodimers constitute the MTs [Sechi and Wehland, 2000; Pelling et al., 2007] and filamins are actin-binding proteins stabilizing the three-dimensional actin filament networks and linking them to cellular membranes [Zhou et al., 2010]. Therefore, the signalling pathway activated by exogenous AIMP1 on ECs could involve these different types of cytoskeletal structure.

The results of experiments in search of AIMP1 interactors, together with the data from the biological assays and immunofluorescence analysis, suggest a possible involvement of proteins controling adhesion and cytoskeletal remodeling in the signaling pathway activated by exogenous AIMP1 in PAEC.

Finally, the phosphoproteomic experiments demonstrated that α-tubulin rapidly gets phosphorylated upon PAEC treatment with AIMP1. The significance of α-tubulin phosphorylation is still under debate. Wandosell et al. [1987] have shown that, when phosphorylated, tubulin does not assemble into polymers and, thus, is not incorporated in MTs. Faruki et al. [2000] showed that phosphorylated tubulin was assembled into MTs only slightly less than untreated tubulin. However, more recently, Fourest-Lieuvin et al. [2006] observed a poor incorporation of phosphorylated tubulin in MTs and concluded that phospho-tubulin has an impaired polymerization capacity. Thus, treatment of PAEC with AIMP1 could impair MT formation by stimulating α-tubulin phosphorylation and interfere with processes such as cellular transport, adhesion, regulation of cell shape, polarity, and motility. Nevertheless, the biological implications of α-tubulin phosphorylation would need to be established.

The fact that the other proteins found to interact with AIMP1 in this study (i.e., vinculin, cingulin, and filamin-A) were not found to be differentially phosphorylated does not mean they do not undergo post-translational modification (PTM) following PAEC stimulation with exogenous AIMP1. They could undergo PTM other than phosphorylation or at time points different from those analyzed in this work. Furthermore, the sensitivity of the 2-DE phosphoproteomic technique may not be high enough to reveal all the four proteins found to interact with AIMP1. In this sense, a more sensitive technique could be used in future studies in order to understand if also vinculin, cingulin, and filamin-A undergo phosphorylation upon PAEC treatment with AIMP1.

In conclusion, on the basis of our results and literature data, we propose a cellular mechanism by which AIMP1 interacts with α5β1 integrin and, upon cell uptake, interacts with a complex composed of at least four cytoskeletal proteins (α-tubulin, vinculin, cingulin, and filamin-A) on the cytosolic face of the cell membrane. Interaction and/or activation of these proteins could regulate cellular architecture maintenance and remodeling.

ACKNOWLEDGMENTS

Research supported in part by Piedmont Region and ISI Foundation.

REFERENCES

Agrawal GK, Thelen JJ. 2005. Development of a simplified, economical polyacrylamide gel staining protocol for phosphoproteins. Proteomics 5:4684–4688.

Carmeliet P. 2005. Angiogenesis in life, disease and medicine. Nature 438:932–936.

Chang SY, Park SG, Kim S, Kang CY. 2002. Interaction of the C-terminal domain of p43 and the alpha subunit of ATP synthase. Its functional implication in endothelial cell proliferation. J Biol Chem 277:8388–8394.

Chesarone MA, DuPage AG, Goode BL. 2010. Unleashing formins to remodel the actin and microtubule cytoskeletons. Nat Rev Mol Cell Biol 11:62–74.

Faruki S, Geahlen RL, Asai DJ. 2000. Syk-dependent phosphorylation of microtubules in activated B-lymphocytes 2. J. Cell Sci 113(Pt 14):2557–2565.

Fourest-Lieuvin A, Peris L, Gache V, Garcia-Saez I, Juillan-Binard C, Lantez V, Job D. 2006. Microtubule regulation in mitosis: Tubulin phosphorylation by the cyclin-dependent kinase Cdk1 2. Mol Biol Cell 17:1041–1050.

Gundersen GG, Cook TA. 1999. Microtubules and signal transduction. Curr Opin Cell Biol 11:81–94.

Guillemot L, Hammar E, Kaister C, Ritz J, Caille D, Jond L, Bauer C, Meda P, Citi S. 2004. Disruption of the cingulin gene does not prevent tight junction formation but alters gene expression. J Cell Sci 117:5245–5256.

Han JM, Park SG, Liu B, Park BJ, Kim JY, Jin CH, Song YW, Li Z, Kim S. 2007. Aminoacyl-tRNA synthetase-interacting multifunctional protein 1/p43 controls endoplasmic reticulum retention of heat shock protein gp96: Its pathological implications in lupus-like autoimmune diseases. Am J Pathol 170:2042–2054.

Jacobs DI, van Rijssen MS, van der HR, Verpoorte R. 2001. Sequential solubilization of proteins precipitated with trichloroacetic acid in acetone from cultured *Catharanthus roseus* cells yields 52% more spots after two-dimensional electrophoresis. Proteomics 1:1345–1350.

Jain RK. 2003. Molecular regulation of vessel maturation. Nat Med 9:685–693.

Janmey PA. 1991. Mechanical properties of cytoskeletal polymers. Curr Opin Cell Biol 3:4–11.

Kao J, Fan YG, Haehnel I, Brett J, Greenberg S, Clauss M, Kayton M, Houck K, Kisiel W, Seljelid R. 1994a. A peptide derived from the amino terminus of endothelial-monocyte-activating polypeptide II modulates mononuclear and polymorphonuclear leukocyte functions, defines an apparently novel cellular interaction site, and induces an acute inflammatory response. J Biol Chem 269:9774–9782.

Kao J, Houck K, Fan Y, Haehnel I, Libutti SK, Kayton ML, Grikscheit T, Chabot J, Nowygrod R, Greenberg S. 1994b. Characterization of a novel tumor-derived cytokine. Endothelial-monocyte activating polypeptide II. J Biol Chem 269:25106–25119.

Keezer SM, Ivie SE, Krutzsch HC, Tandle A, Libutti SK, Roberts DD. 2003. Angiogenesis inhibitors target the endothelial cell cytoskeleton through altered regulation of heat shock protein 27 and cofilin. Cancer Res 63: 6405–6412.

Kim Y, Kim JE, Lee SD, Lee TG, Kim JH, Park JB, Han JM, Jang SK, Suh PG, Ryu SH. 1999. Phospholipase D1 is located and activated by protein kinase C alpha in the plasma membrane in 3Y1 fibroblast cell. Biochim Biophys Acta 1436:319–330.

Kim S, Bell K, Mousa SA, Varner JA. 2000a. Regulation of angiogenesis in vivo by ligation of integrin alpha5beta1 with the central cell-binding domain of fibronectin. Am J Pathol 156:1345–1362.

Kim Y, Shin J, Li R, Cheong C, Kim K, Kim S. 2000b. A novel anti-tumor cytokine contains an RNA binding motif present in aminoacyl-tRNA synthetases. J Biol Chem 275:27062–27068.

Knies UE, Behrensdorf HA, Mitchell CA, Deutsch U, Risau W, Drexler HC, Clauss M. 1998. Regulation of endothelial monocyte-activating polypeptide II release by apoptosis. Proc Natl Acad Sci USA 95:12322–12327.

Ko YG, Park H, Kim T, Lee JW, Park SG, Seol W, Kim JE, Lee WH, Kim SH, Park JE, Kim S. 2001. A cofactor of tRNA synthetase, p43, is secreted to up-regulate proinflammatory genes. J Biol Chem 276:23028–23033.

Laemmli UK. 1970. Cleavage of structural proteins during the assembly of the head of bacteriophage T4. Nature 227:680–685.

Lee YS, Han JM, Kang T, Park YI, Kim HM, Kim S. 2006. Antitumor activity of the novel human cytokine AIMP1 in an in vivo tumor model. Mol Cells 21:213–217.

Liu S, Tobias R, McClure S, Styba G, Shi Q, Jackowski G. 1997. Removal of endotoxin from recombinant protein preparations. Clin Biochem 30:455–463.

Marchetti-Deschmann M, Kemptner J, Reichel C, Allmaier G. 2009. Comparing standard and microwave assisted staining protocols for SDS-PAGE of glycoproteins followed by subsequent PMF with MALDI MS. J Proteomics 72:628–639.

Mendes KN, Wang GK, Fuller GN, Zhang W. 2010. NK mediates insulin-like growth factor binding protein 2/integrin alpha5-dependent glioma cell migration. Int J Oncol 37(1):143–153.

Mila S, Albo AG, Corpillo D, Giraudo S, Zibetti M, Bucci EM, Lopiano L, Fasano M. 2009. Lymphocyte proteomics of Parkinson's disease patients reveals cytoskeletal protein dysregulation and oxidative stress. Biomark Med 3:117–128.

Park SG, Jung KH, Lee JS, Jo YJ, Motegi H, Kim S, Shiba K. 1999. Precursor of pro-apoptotic cytokine modulates aminoacylation activity of tRNA synthetase. J Biol Chem 274:16673–16676.

Park H, Park SG, Kim J, Ko YG, Kim S. 2002a. Signaling pathways for TNF production induced by human aminoacyl-tRNA synthetase-associating factor, p43. Cytokine 20:148–153.

Park H, Park SG, Lee JW, Kim T, Kim G, Ko YG, Kim S. 2002b. Monocyte cell adhesion induced by a human aminoacyl-tRNA synthetase-associated factor, p43: Identification of the related adhesion molecules and signal pathways. J Leukoc Biol 71:223–230.

Park SG, Kang YS, Ahn YH, Lee SH, Kim KR, Kim KW, Koh GY, Ko YG, Kim S. 2002c. Dose-dependent biphasic activity of tRNA synthetase-associating factor, p43, in angiogenesis. J Biol Chem 277:45243–45248.

Park SG, Ewalt KL, Kim S. 2005a. Functional expansion of aminoacyl-tRNA synthetases and their interacting factors: New perspectives on housekeepers. Trends Biochem Sci 30:569–574.

Park SG, Shin H, Shin YK, Lee Y, Choi EC, Park BJ, Kim S. 2005b. The novel cytokine p43 stimulates dermal fibroblast proliferation and wound repair. Am J Pathol 166:387–398.

Pelling AE, Dawson DW, Carreon DM, Christiansen JJ, Shen RR, Teitell MA, Gimzewski JK. 2007. Distinct contributions of microtubule subtypes to cell membrane shape and stability. Nanomedicine 3:43–52.

Quevillon S, Agou F, Robinson JC, Mirande M. 1997. The p43 component of the mammalian multi-synthetase complex is likely to be the precursor of the endothelial monocyte-activating polypeptide II cytokine. J Biol Chem 272: 32573–32579.

Revenu C, Athman R, Robine S, Louvard D. 2004. The co-workers of actin filaments: From cell structures to signals. Nat Rev Mol Cell Biol 5:635–646.

Schwarz MA, Kandel J, Brett J, Li J, Hayward J, Schwarz RE, Chappey O, Wautier JL, Chabot J, Lo GP, Stern D. 1999. Endothelial-monocyte activating polypeptide II, a novel antitumor cytokine that suppresses primary and metastatic tumor growth and induces apoptosis in growing endothelial cells. J Exp Med 190:341–354.

Schwarz MA, Zheng H, Liu J, Corbett S, Schwarz RE. 2005. Endothelial-monocyte activating polypeptide II alters fibronectin based endothelial cell adhesion and matrix assembly via alpha5 beta1 integrin. Exp Cell Res 311:229–239.

Sechi AS, Wehland J. 2000. The actin cytoskeleton and plasma membrane connection: PtdIns(4,5)P(2) influences cytoskeletal protein activity at the plasma membrane. J Cell Sci 113(Pt 21):3685–3695.

Sen T, Dutta A, Maity G, Chatterjee A. 2010. Fibronectin induces matrix metalloproteinase-9 (MMP-9) in human laryngeal carcinoma cells by involving multiple signaling pathways. Biochimie 92(10):1422–1434.

Shalak V, Kaminska M, Mitnacht-Kraus R, Vandenabeele P, Clauss M, Mirande M. 2001. The EMAPII cytokine is released from the mammalian multisynthetase complex after cleavage of its p43/proEMAPII component. J Biol Chem 276:23769–23776.

Stevenson BR, Heintzelman MB, Anderson JM, Citi S, Mooseker MS. 1989. ZO-1 and cingulin: Tight junction proteins with distinct identities and localizations. Am J Physiol 257:C621–C628.

Stossel TP. 1993. On the crawling of animal cells. Science 260:1086–1094.

Wandosell F, Serrano L, Avila J. 1987. Phosphorylation of alpha-tubulin carboxyl-terminal tyrosine prevents its incorporation into microtubules 3. J Biol Chem 262:8268–8273.

Yan XD, Pan LY, Yuan Y, Lang JH, Mao N. 2007. Identification of platinum-resistance associated proteins through proteomic analysis of human ovarian cancer cells and their platinum-resistant sublines. J Proteome Res 6:772–780.

Yi JS, Lee JY, Chi SG, Kim JH, Park SG, Kim S, Ko YG. 2005. Aminoacyl-tRNA synthetase-interacting multi-functional protein, p43, is imported to endothelial cells via lipid rafts. J Cell Biochem 96:1286–1295.

Zhou AX, Hartwig JH, Akyurek LM. 2010. Filamins in cell signaling, transcription and organ development. Trends Cell Biol 20:113–123.

Zhu C, Bao G, Wang N. 2000. Cell mechanics: Mechanical response, cell adhesion, and molecular deformation. Annu Rev Biomed Eng 2: 189–226.